Journal of Thermal Analysis and Calorimetry (2021) 143:2893–2900
https://doi.org/10.1007/s10973-019-09205-5

Comparative study of the thermal behavior of Sr–Cu–O gels obtained by sol–gel and microwave-assisted sol–gel method

Luminita Predoana[1] · Irina Atkinson[1] · Dániel Attila Karaj[2] · Vincent Otieno Odhiambo[2] · László Péter Bakos[2] · Teodóra Nagyné Kovács[2] · Jeanina Pandele-Cusu[1] · Simona Petrescu[1] · Adriana Rusu[1] · Imre M. Szilágyi[2] · György Pokol[2,3] · Maria Zaharescu[1]

Received: 18 November 2019 / Accepted: 16 December 2019 / Published online: 23 January 2020

Abstract
In the literature data, several papers reported the synthesis by various chemical or physical methods of the $SrCu_2O_2$ (SCO) having possible applications in thermoelectric or completely electronic devices such as solar cells, liquid crystal displays and touch screen. A great challenge is represented by the formation of the pure $SrCu_2O_2$ (SCO), due to the high labiality of the Cu valence, depending on temperature. In the present paper, the thermal behavior of Sr–Cu–O gels obtained by sol–gel (SG) or microwave (MW)-assisted SG methods was studied in order to establish the appropriate thermal conditions for pure nanostructured $SrCu_2O_2$ preparation. As reagents, copper and strontium acetylacetonate in alcoholic media were used. The starting solutions were homogenized either by stirring for 2 h at room temperature or were exposed to MW for 5 min at 300 W and a frequency of 2.45 GHz. Both solutions were left to gel at room temperature. The obtained gels were investigated by scanning electron microscopy, Fourier-transform infrared spectroscopy, as well as by thermal analysis combined with evolved gas analysis (TG/DTA-MS) measurements in air, inert and reducing atmospheres. For both type of samples, a stepwise thermal decomposition of the gels was noticed in a large temperature range. In the case of samples obtained by microwave-assisted SG method, a higher number of thermal effects were registered assigned to a higher number of molecular species formed in the sample. The residues obtained by non-isothermal treatment up to 900 °C, of both type of samples, were investigated by X-ray diffraction. The results demonstrate the influence of the MW on the SG synthesis and on the thermal properties of the resulted gels. Based on the obtained results, the required thermal treatment of the gels in order to obtain convenient precursors powders for obtaining pure $SrCu_2O_2$ could be proposed.

Keywords $SrCu_2O_2$ · Sol–gel · Microwave · Synthesis · Thermal treatment

Introduction

High-Tc superconductivity in complex copper oxides was one of the greatest discoveries of the last century. Most of the copper oxide superconductors possess a multilayered crystal structure. This discovery initiated massive research not only on new superconducting materials, but also on many related fields, involving multilayered transition metal oxide materials as transparent conducting oxides (TCO) with applications in flat panel displays, photovoltaic cells, low-e windows and organic optoelectronic devices [1].

Among the TCO materials, Cu_2SrO_2 has been identified as a dopeable p-type non-delafossite TCO with synthesis temperatures as low as 400 °C [2–4].

For obtaining $SrCu_2O_2$ transparent conducting oxides, several methods of preparation were used. Among the

✉ Imre M. Szilágyi
imre.szilagyi@mail.bme.hu

✉ Maria Zaharescu
mzaharescu2004@gmail.com

[1] "Ilie Murgulescu" Institute of Physical Chemistry, Romanian Academy, 202 Splaiul Independentei, 060021 Bucharest, Romania

[2] Department of Inorganic and Analytical Chemistry, Budapest University of Technology and Economics, Műegyetem rakpart 3, Budapest 1111, Hungary

[3] Research Center for Natural Sciences, Hungarian Academy of Science, Magyar tudósok körútja 2, Budapest 1117, Hungary

physical methods of $SrCu_2O_2$ synthesis, the pulsed laser deposition was mainly approached [5–11].

Chemical methods of $SrCu_2O_2$ preparation are less studied. First chemical methods mentioned in the literature refer to chemical vapor deposition (CVD) [12] and metal-organic chemical vapor deposition (MO-CVD) [13]. Among the chemical methods in liquid phase, sol–gel technique is a versatile and efficient method for pure or doped metal oxide films or powders preparation [14–17], showing some advantages over other preparation techniques. Such benefits are purity, homogeneity, possibility to introducing dopants in large quantities, ease of manufacturing, low processing temperature, control over the stoichiometry, composition, viscosity [18, 19]. According to Ginley et al. [20], the first study of $SrCu_2O_2$ preparation by chemical method and solutions depositions was published in 2003.

Combining the sol–gel method with the effect of ultrasounds or microwaves leads to improving the sol–gel procedure [21–24]. Microwaves are electromagnetic radiations with wavelengths ranging from 1 mm to 1 m with frequencies between 300 MHz (100 cm) and 300 GHz (0.1 cm). Microwave heating mechanism is based on interactions between dipoles in materials and the electromagnetic microwaves. Microwave heating has certain benefits over conventional ovens, as: reaction rate acceleration, milder reaction conditions, higher chemical yield, lower energy usage, different reaction selectivity [25, 26].

In the present paper, the thermal behavior of the Sr–Cu–O gels obtained by sol–gel (SG) and microwave (MW)-assisted sol–gel methods is approached in order to establish the most appropriate experimental conditions for obtaining precursor powders for pure $SrCu_2O_2$ compound preparation.

Experimental

Sample preparation

The reagents used for the sample preparation were 0.25 molar solutions of strontium acetyl acetonate (SrAcAc, $Sr(C_5H_7O_2)_2$ Alfa Aesar 99.99%) as strontium source and copper(II) acetyl acetonate (CuAcAc, $Cu(C_5H_7O_2)_2$ Merck ≥ 99.0%) as cooper source in ethanol (C_2H_5OH, absolute, Merck), as solvent. The triethanolamine (TEA, $N(C_2H_4OH)_3$, Merck 99%) has the role of the chelating agent and was used in a molar ratio reagents:chelating agent = 1:1.

In the case of sol–gel (SG) method, the starting solution was homogenized under vigorous stirring for 2 h at 80 °C. The resulted sample was noted: Sr–Cu–O (SG).

In the case of microwave (MW)-assisted sol–gel method, the same starting solution was homogenized by stirring and exposing to microwaves (MW) for 5 min at 300 W and a frequency of 2.45 GHz. The resulted solution was noted: Sr–Cu–O (MW).

Methods of characterization

The synthesized samples were investigated by scanning electron microscopy (SEM) using a high-resolution microscope, FEI Quanta 3D FEG model, operating at 30 kV.

Fourier-transform infrared spectroscopic (FT-IR) investigations were realized using a Nicolet Spectrometer Nico 6700 FT-IR between 400 and 4000 cm^{-1}. The spectra of the gels were obtained using the KBr pellet technique. The spectra were recorded at a resolution of 4 cm^{-1}.

The differential thermal and thermo-gravimetric analysis coupled with mass spectrometry TG/DTA-MS was studied by a STD 2960 simultaneous DTA/TGA (TA Instruments Inc.) thermal analyzer using a heating rate of 10 °C min^{-1} and Pt crucibles. The investigations were realized in air, N_2 and 5% H_2/95% Ar atmospheres. Evolved gas analytical (EGA) curves were recorded by a Thermostar GSD 200 (Balzers Instruments) quadrupole mass spectrometer (MS). A mass range between m/z = 1–64 was monitored through 64 channels in multiple ion detection mode (MID) with a measuring time of 0.5 s $channel^{-1}$. On-line coupling between the TG/DTA and MS devices was achieved by a heated (T = 200 °C), 100% methyl deactivated fused silica capillary tube with inner diameter of 0.15 mm.

The powder X-ray diffraction (XRD) patterns were measured with a PANalytical X'pert Pro MPD X-ray diffractometer using Cu Kα irradiation. The patterns were collected using a Si single crystal sample holder.

Results and discussion

In the experimental conditions presented above, pieces of gels of different size and blueish-green color were obtained for both preparation methods (Fig. 1).

The FT-IR spectra of the prepared samples are presented in Fig. 2a, b, and the vibration bands are shown comparatively, in Table 1. In the case of both samples, many similar vibration peaks were recorded, but with different intensities. FT-IR spectra of the samples show small intensity vibrations of Sr–O and Cu–O and high intensity vibrations for organic and hydroxyl species [27].

Broad absorption bands between 3500 and 3200 cm^{-1} indicate the presence of the hydroxyl groups, adsorbed water and amine groups [28, 29]. The band around 1380 cm^{-1} is assigned to the amine group's vibration, and the band at 1626 cm^{-1} is assigned to the bending vibration of the molecular water.

The bands around 825 and 593 cm^{-1} could be attributed to vibration of Sr–O [30], and the band at 508 cm^{-1} is

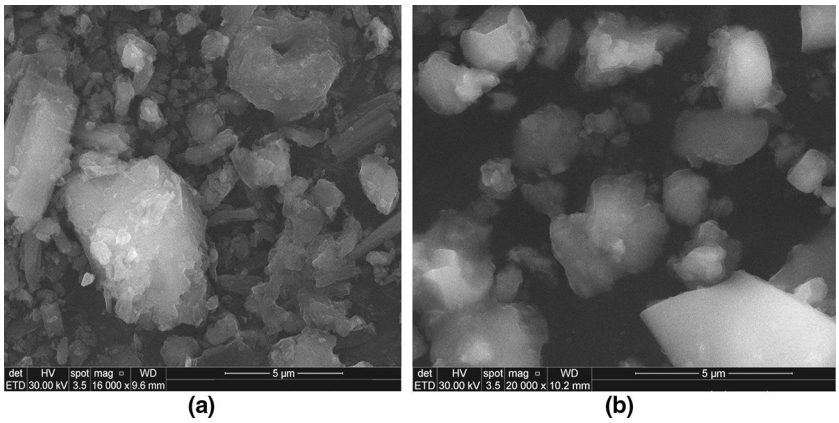

Fig. 1 SEM images of the synthesized samples obtained by **a** sol–gel method and **b** by MW-assisted sol–gel method

assigned to the Sr–O–Cu vibration [31] from the precursor powder. At lower wavelength values, the vibrational bands of metal oxygen bonds are presented with a weak intensity.

A higher number of vibration bands are observed for the samples obtained by MW-assisted sol–gel method, assigned to the presence of higher number of molecular species in the compositions of the samples.

The thermal analysis of the synthesized samples was realized in three different atmospheres (air, N_2 and 5%H_2/95%Ar) in order to establish their influence on the decomposition process. For the samples synthesized by sol–gel method, the TG/DTA and corresponding MS results are presented in Figs. 3–5.

The TGA–DTA curves for the samples thermally treated in air show the presence of two main and a third smaller decomposition steps. The first decomposition occurs between 150 and 250 °C being assigned to the elimination of the adsorbed water and structural organic part of the as-prepared sample and the second one is at about 250–450 °C, being correlated to the overlap of two effects: the elimination of the organic residue and their subsequent oxidation. Between 450 and 700 °C, there is no mass loss. Above this temperature, a small mass increse is possible do to the oxidation of mettalic species that could be formed during the decomposition of the sample. The third mass loss step takes place between 800 and 900 °C. The total mass loss of these three decomposition steps was 66.85%. The MS curves sustain the mentioned assignments. The species shown on the MS spectra could be assigned to the following fragments: 18: H_2O^+; 30: C_2H_6 or can be NO^+, 44: CO_2^+, 46: $C_2H_5OH^+$ or can be NO_2^+. The presence of 30 and 46 fragments in the evolved gases and their assignment to NO or NO_2, species could be explained by the presence of the triethanolamine (TEA) in high amount in the reaction mixture. They could be formed either by oxidation by the annealing atmosphere or by some internal oxidation reactions in the solid state.

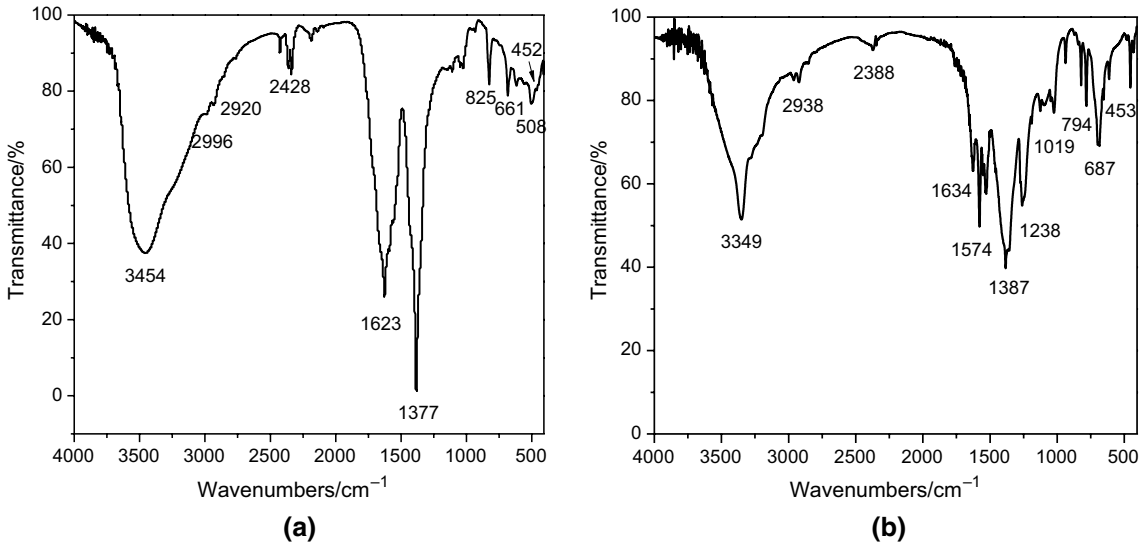

Fig. 2 The FT-IR spectra of the synthesized samples by **a** sol–gel method, **b** MW-assisted sol–gel method

Table 1 FT-IR vibration band of the samples prepared by sol–gel and MW-assisted sol–gel method

Wavenumber/cm^{-1}		Assignments and vibration modes
Sr–Cu–O (SG)	Sr–Cu–O (MW)	
452	453	Cu–O
508	–	Sr–O–Cu
–	593	Sr–O
661	687	C–H
–	794	C–H
825	–	Sr–O
–	930	C–H
–	1019	C–O
–	1238	C–O–C
1377	1387	Amine group
–	1528	ν_{as} (CO), C–H
–	1574	$C{=}O_{as}$
1623	1634	ν_s (OH) in water
2428	2388	CO_3^{2-}
2920	2938	C–H, ν_{as} $(CH)_3$
2996	–	Amine group
–	3349	Amine group
3454	–	H–O–H

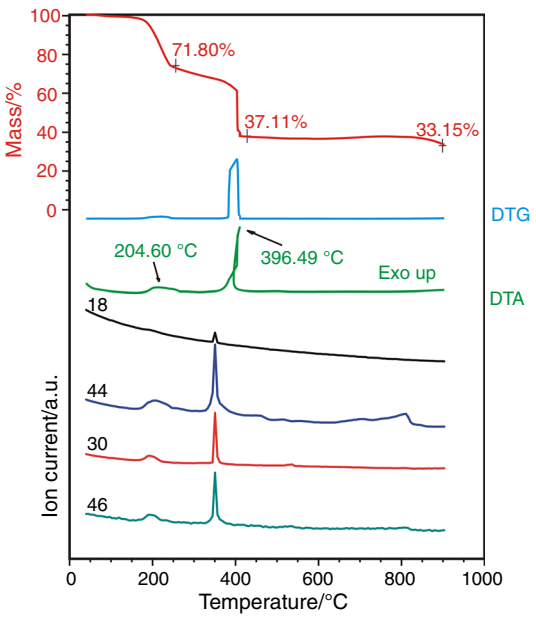

Fig. 3 Thermal decomposition curves *in air* for the sample synthesized by sol–gel method

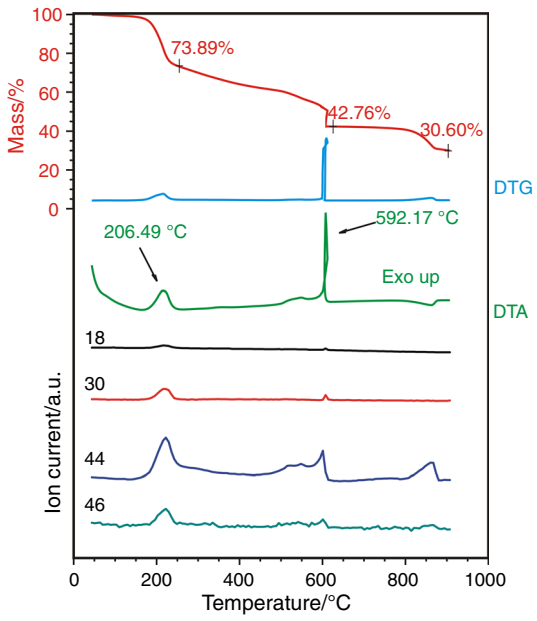

Fig. 4 Thermal decomposition curves *in* N_2 for the sample synthesized by sol–gel method

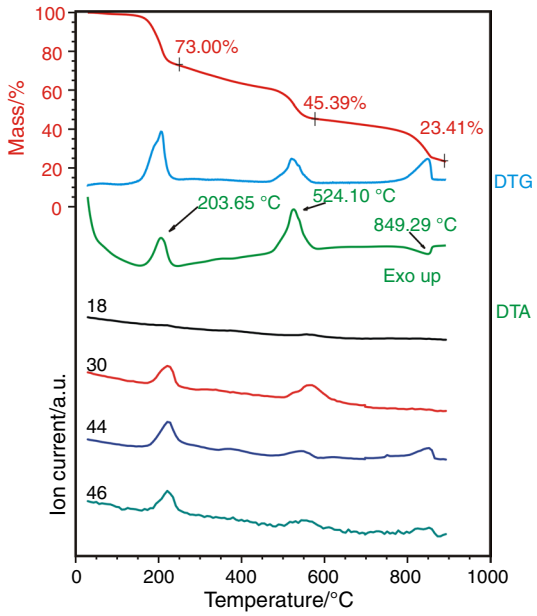

Fig. 5 Thermal decomposition curves *in 5%H_2/95%Ar* for the sample synthesized by sol–gel method

For the sample thermally treated in inert atmosphere (N_2), the decomposition takes place also in three main steps. The first step is similar; however, the second mass loss is composed of overlapping processes. At first, an elongated mass loss begins, related to the decomposition and elimination of the carbonaceous residue. At the end of the second mass loss, some internal or external oxidation could have taken place, resulting in a sharp mass loss around 590 °C. Also in contrast to air, the third mass loss step is more defined in N_2. In N_2, the evolution of the same gases was observed, as mentioned before (H_2O^+; C_2H_6 and NO^+, CO_2^+, 46: $C_2H_5OH^+$ and NO_2^+). The final mass loss in inert atmosphere

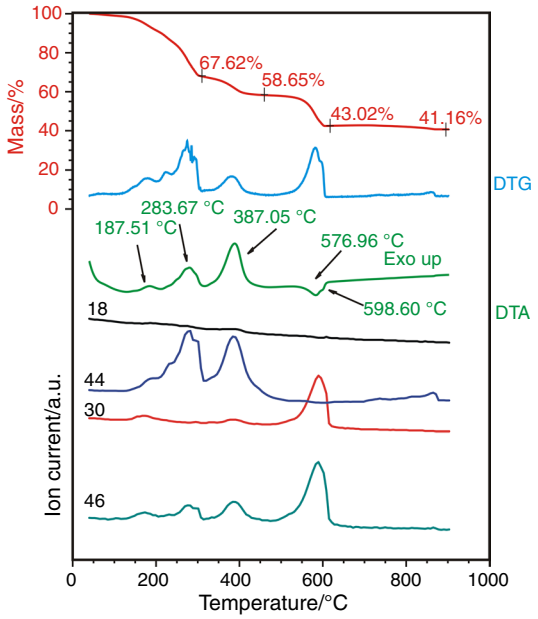

Fig. 6 Thermal decomposition curves *in air* for the sample synthesized by MW-assisted sol–gel method

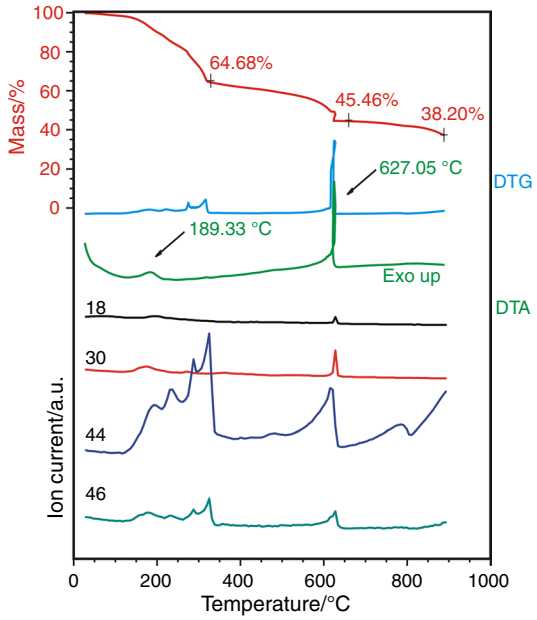

Fig. 7 Thermal decomposition curves *in* N_2 for the sample synthesized by MW-assisted sol–gel method

is higher by 3% (69.40% instead of 66.85%) than in air, which is explained by that in inert atmosphere the small mass increase above 700 °C due to the oxidation metallic species was missing.

In the case of the reductive atmosphere, the decomposition takes place in three main steps with the evolution of all four gases identified in the case of the decomposition of the gel in air and inert atmosphere (H_2O^+; C_2H_6 and NO^+, CO_2^+, $C_2H_5OH^+$ and NO_2^+). The complete mass loss is highest in the case of the sample annealed in reducing atmosphere, which is rationalized by that reduction (decrease in the oxidation number) of the oxides takes place.

The DTA curve shows endothermic heat effects for decomposition processes; however, in air, this is soon overcompensated by the combustion of the organic species, making the DTA peaks exothermic. However, exothermic heat effects are present both in inert and reducing atmospheres at around 210–220 °C and 500–600 °C, pointing to that the process here is exothermic independent on the atmosphere. Most probably here some spontaneous ordering of the solid structure, or some inter- or intramolecular oxidation and combustion steps with the involvement of the organic material, i.e., combustion processes among the oxygen-containing decomposition products and hydrocarbon moieties can take place.

In the case of thermal decomposition in air of the sample synthesized by MW-assisted sol–gel method, Sr–Cu–O (MW) (Fig. 6), four mass loss steps are visible, instead of three as in the case of the sol–gel sample. The total mass is 58.84%, which is considerably less than for the sol–gel sample, and this shows the higher stability of the intermediates of the MW sample. Furthermore, there are more pronounced overlapping processes and with higher number, revealing the more complex nature of the thermal decomposition of the MW sample. As a further new feature, there is an endothermic heat effect around 570–600 °C, most probably belonging to some decomposition processes, as

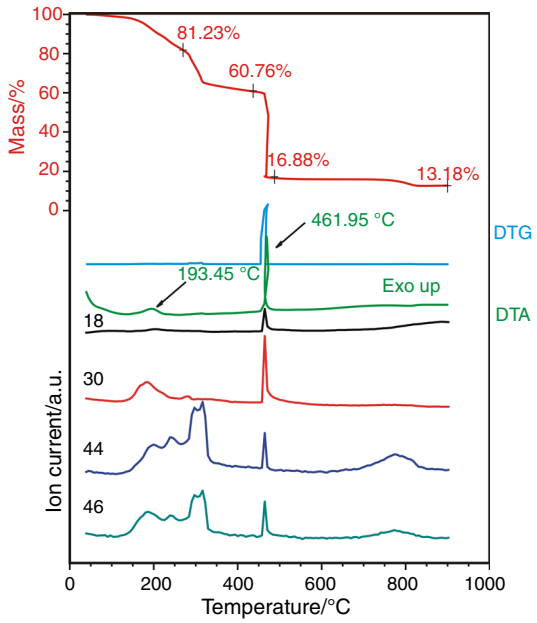

Fig. 8 Thermal decomposition curves *in* $5\%H_2/95\%Ar$ for the sample synthesized by MW-assisted sol–gel method

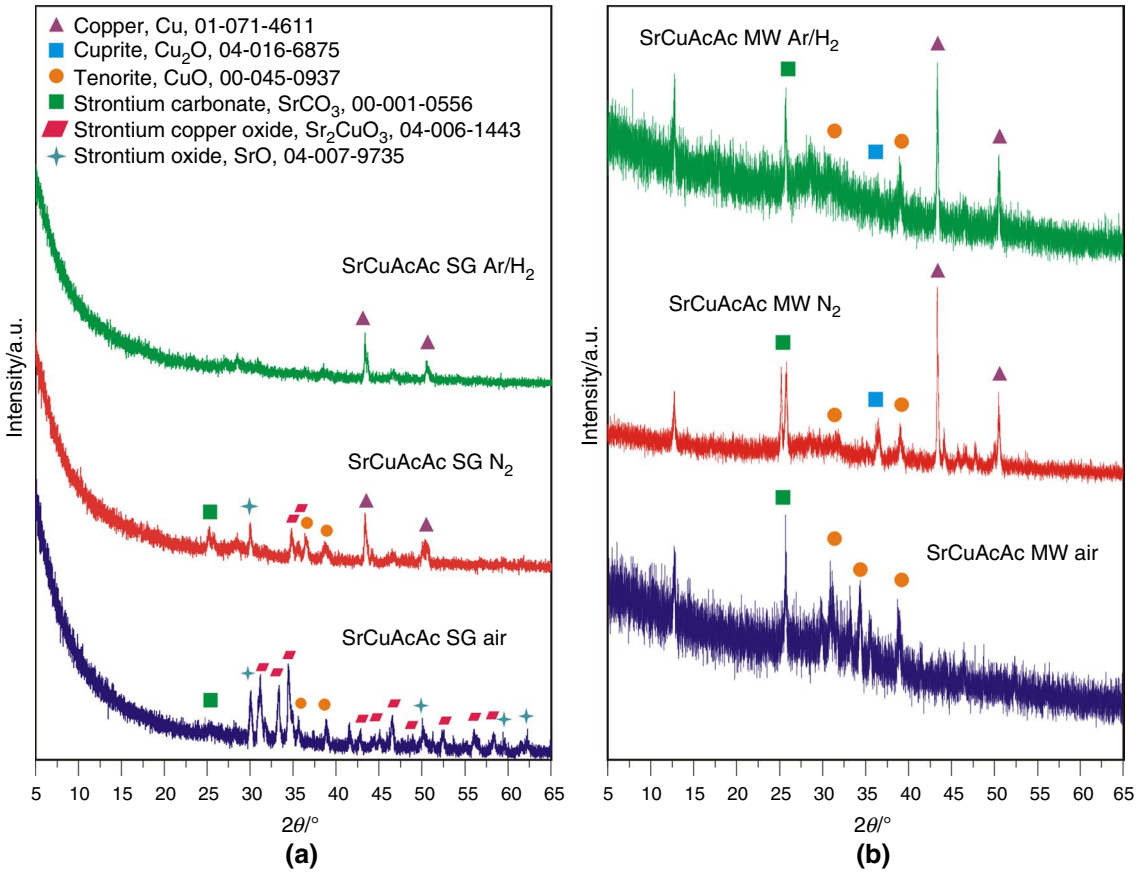

Fig. 9 XRD patterns of the **a** sol–gel and **b** MW-assisted sol–gel samples annealed at 900 °C in air, N_2 and 5%H_2/95%Ar with ICDD card number

revealed by the detection of $C_2H_6^+$ and $C_2H_5OH^+$ fragments by the MS.

The thermal decomposition of the MW sample in N_2 (Fig. 7) is more similar to the sol–gel sample annealed in inert atmosphere. The previous decomposition and internal oxidation processes accompanied by exothermic heat effects around 200 °C and 600 °C were observed here as well. However, there were more pronounced overlapping processes here as well, similar to the MW sample annealed in air. The residual mass is again lower for the MW sample in N_2, than for the sol–gel sample. On the other hand, similar to the sol–gel sample, the mass of the residue of the MW sample annealed in air is higher than in N_2.

The thermal decomposition of the MW sample happens mostly in a similar way in reducing atmosphere (Fig. 8) as in inert one, until 400 °C. Then, as a considerably difference, compared to the MW sample annealed in N_2 and also to the sol–gel sample heated in reducing atmospheres, the second major mass loss step accompanied by the sharp exothermic heat effect happens at ca. 100–150 °C lower temperatures. Most probably, the involvement of H_2 accelerates the inter- or intramolecular combustion steps and this is also supported by that the residual mass is lowest for the MW sample annealed in reducing atmospheres, among all the studied sol–gel and MW samples.

The results obtained by TG/DTA-MS investigations put in evidence the influence of MW on the sol–gel synthesis leading to more complex compositions of the resulted gels that contain higher number of molecular species with higher thermal stability. In the case of MW treated samples, more decomposition steps were observed. A similar behavior was observed in the case of V-doped TiO_2 gels obtained by MW-assisted sol–gel method [32]. The results are in agreement with the FT-IR results that also identified more vibration bands for the samples obtained by MW sol–gel method.

Most commonly, the thermal treatments of the sol–gel synthesized materials are done in air atmosphere, in order to eliminate and burn out the organic part from their compositions. However, our studies show that complementary studies in both inert and reducing atmospheres are also useful, as they carry additional information about the starting materials.

The X-ray diffraction spectra for the heated samples obtained by sol–gel and MW-assisted sol–gel method are

presented in Fig. 9a, b, respectively. Based on the XRD study of the sol–gel sample, the final product is composed of a mixture of phases. The main component is $SrCu_2O_3$. Besides that SrO and CuO are present in considerable amounts, and only traces of $SrCO_3$ can be detected. When the sample is annealed in inert atmosphere, due to the missing oxidizing atmosphere, the amount of $SrCu_2O_3$, SrO and CuO becomes smaller and Cu metal appears in significant amount. Traces of $SrCO_3$ can be still observed. Under reducing conditions, the residue is almost completely dominated by Cu, and all the other phases can be also guessed in tiny quantities.

The XRD pattern of the MW sample annealed in air shows that the residue is composed of CuO, revealing complete oxidation of Cu. Similar to the sol–gel sample, traces of Sr-carbonate are also observed. When the sample was annealed in inert atmosphere, beside CuO, Cu_2O and Cu also appeared, revealing the partially reduced status of the Cu atom. When the heating was done in reducing atmosphere, the main product was copper metal.

In the case of the samples synthesized by MW-assisted sol–gel method, for all atmospheres in which the thermal treatment was done, powders with lower degree of crystallization were obtained, leading to the conclusion that in the presence of the MW during the sol–gel process, higher number of molecular species with higher thermal stability and consequently lower tendency of crystallization were formed. The decomposition sequences of the sol–gel and MW samples have similarities, but also differences, as revealed previously by TG/DTA-MS and now by XRD. In the case of the sol–gel sample annealed in air, Sr–Cu–O phase was also present, while the MW sample heated in air had CuO as main component. In the case of the MW sample, partially reduced copper oxide was also observed, as an intermediate between CuO and Cu.

Differences regarding the formation of CuO-based compounds prepared in the presence of microwaves were also previously mentioned [33].

Conclusions

Nanosized powders in the Sr–Cu–O system were obtained by sol–gel and microwave-assisted sol–gel methods, starting with acetylacetonates, in alcoholic medium. The thermal decomposition of both types of samples was studied in air, N_2 and $5\%H_2/95\%Ar$ atmosphere, and in all cases, a complex decomposition takes place.

The synthesis of the samples by microwave-assisted sol–gel method increases the complexity, and the thermal stability of the molecular species formed, as shown by TG/DTA-MS measurements.

The X-ray diffraction study of the residues of the thermal treatment has shown different structures of the samples. In the case of MW-assisted sol–gel method, samples with lower degree of crystallization were obtained. When the sol–gel sample was annealed in air, $SrCu_2O_3$ was the main constituent. In contrast, the MW sample annealed in air was dominated by CuO. When the thermal treatment was done in inert or reducing atmospheres, the presence of Cu was also identified.

Powders prepared in the conditions discussed in the paper could be used as precursors for $SrCu_2O_2$ preparation by supplementary thermal treatment in H^2 atmosphere or in high vacuum.

Acknowledgements Open access funding provided by Budapest University of Technology and Economics (BME). This work was performed in the frame of mobility Project "Reduced semiconductor oxides for TCO, photocatalysis and gas sensing applications", 2019–2021, between Ilie Murgulescu Institute of Physical Chemsitry of the Romanian Academy Bucharest, Romania and Research Center of Natural Sciences, Hungarian Academy of Science Research Group of the Hungarian Academy of Science at the Budapest, Hungary. We acknowledge as well the support of the EU (ERDF) and Romanian Government that allowed for the acquisition of the research infrastructure under POS-CCE O 2.2.1 project INFRANANOCHEM—No. 19/01.03.2009. A GINOP-2.2.1-15-2017-00084, an NRDI K 124212, an NRDI TNN_16 123631 and an NRDI K 128266 grants are acknowledged. The work performed within project VEKOP-2.3.2-16-2017-00013 was supported by the European Union and the State of Hungary, co-financed by the European Regional Development Fund. The research reported in this paper was supported by the Higher Education Excellence Program of the Ministry of Human Capacities in the frame of Nanotechnology and Materials Science research area of Budapest University of Technology (BME FIKP-NAT).

References

1. Ginley DS, Bright C. Transparent conducting oxides. MRS Bull. 2000;25:15–8.
2. Ohta H, Orita M, Hirano M, Yagi I, Ueda K, Hosono H. Electronic structure and optical properties of $SrCu_2O_2$. J Appl Phys. 2002;91:3074–8.
3. Ohta H, Orita M, Hirano M, Ueda K, Hosono H. Epitaxial growth of transparent conductive oxides. Int J Mod Phys B. 2002;16:173–80.

4. Robertso J, Peacock PW, Towler MD, Needs R. Electronic structure of p-type conducting transparent oxides. Thin Solid Films. 2002;411:96–100.
5. Kudo A, Yanagi H, Hosono H, Kawazoe H. $SrCu_2O_2$: $SrCu_2O_2$: a p-type conductive oxide with wide band gap. Appl Phys Lett. 1998;73:220–2.
6. Varadarajan V, Norton DP, Budai JD. Phase stability and orientation of $SrCu_2O_2$ films grown by pulsed laser deposition. Thin Solid Films. 2005;488:173–7.
7. Tambunan OT, Tukiman H, Parwanta KJ, JeongDW JungCU, Rhee SJ, Liu C. Structural and optical properties of $SrCu_2O_2$ films deposited on sapphire substrates by pulsed laser deposition. Superlattices Microstruct. 2012;52:774–81.
8. Ohta H, Kawamura KI, Orita M, Hirano M, Sarukura N, Hosono H. Current injection emission from a transparent p–n junction composed of p–$SrCu_2O_2$/n–ZnO. Appl Phys Lett. 2000;77:475–7.
9. Zhang N, Sun J, Gong H. Transparent p-type semiconductors: copper-based oxides and oxychalcogenides. Coatings. 2019;9:137–64.
10. Hwang D-K, Oh M-S, Lim J-H, Kang C-G, Park S-J. Effect of annealing temperature and ambient gas on phosphorus doped p-type ZnO. Appl Phys Lett. 2007;90:021106.
11. Li CX, Lai PT, Xu JP. Improved reliability of Ge MOS capacitor with HfTiON high-k dielectric by using Ge surface pretreatment in wet NO. In: IEEE conference on electron devices and solid-state circuits; 2007. p. 185–8.
12. Sakka S. Sol–gel process and applications. Handbook of advanced ceramics. Amsterdam: Elsevier; 2013. p. 883–910.
13. Schmidt H. Chemistry of material preparation by the sol–gel process. J Non-Cryst Solids. 1988;100:51–64.
14. Brinker CJ, Scherer GW. Sol–gel science: the physics and chemistry of sol–gel processing. San Diego: Academic Press; 1990.
15. Wang D, Bierwagen GP. Sol–gel coatings on metals for corrosion protection. Prog Org Coat. 2009;64:327–38.
16. Alcock CB, Li B. Thermodynamic study of the Cu–Sr–O system. J Am Ceram Soc. 1990;73:1176–80.
17. Suzuki RO, Bohac P, Gauckleret LJ. Thermodynamics and phase equilibria in the Sr–Cu–O system. J Am Ceram Soc. 1992;75:2833–42.
18. Livage J, Henry H, Sanchez C. Sol–gel chemistry of transition metal oxides. Prog Solid State Chem. 1988;18:259–341.
19. Akpan UG, Hameed BH. The advancements in sol–gel method of doped-TiO_2 photocatalysts—a review. Appl Catal A Gen. 2010;375:1–11.
20. Ginley D, Roy DB, Ode A, Warmsingh C, Yoshida Y, Parilla P, Teplin C, Kaydanova T, Miedaner A, Curtis C, Martinson A, Coutts T, Readey D, Hosono H, Perkins J. Non-vacuum and PLD growth of next generation TCO materials. Thin Solid Films. 2003;445:193–8.
21. Fetter G, Bosch P, Lopez T. ZrO_2 and Cu/ZrO_2 sol–gel synthesis in presence of microwave irradiation. J Sol Gel Sci Technol. 2002;23:199–203.
22. Dwivedi R, Maurya A, Verma A, Prasad R, Bartwal KS. Microwave assisted sol–gel synthesis of tetragonal zirconia nanoparticles. J Alloys Compd. 2011;509:6848–51.
23. Jaimy KB, Vidya K, Saraswathy HUN, Hebalkar NY, Warrier KGK. Dopant-free anatase titanium dioxide as visible-light catalyst: facile sol–gel microwave approach. J Environ Chem Eng. 2015;3:1277–86.
24. Kharade RR, Patil KR, Patil PS, Bhosale PN. Novel microwave assisted sol–gel synthesis (MW-SGS) and electrochromic performance of petal like h-WO_3 thin films. Mater Res Bull. 2012;47:1787–93.
25. Predoana L, Stanciu I, Zaharescu M. Advances in microelectronics: reviews', book series, metal oxide nanomaterials obtained by sol–gel and microwave assisted sol–gel methods. Barcelona: IFSA Publishing; 2019. p. 221–49.
26. Li Y, Yang W. Microwave synthesis of zeolite membranes: a review. J Membr Sci. 2008;316:3–17.
27. Zaharescu M, Mocioiu OC. Infrared Spectroscopy. In: Schneller T, Waser R, Kosec M, Payne D, editors. Chemical solution deposition of functional oxide thin films. Wien: Springer; 2013. p. 213–30.
28. Coate J. Interpretation of infrared spectra. A practical approach. In: Meyers RA, editor. Encyclopedia of analytical chemistry. London: Wiley; 2006. p. 10815–37.
29. Nakamoto K. Infrared and Raman spectra of inorganic and coordination compounds. 4th ed. New York: Wiley; 1986.
30. Rahman MM, Asiri MA, Hussain MM. A novel approach towards the hydrazine sensor development by SrO·CNT nanocomposites. RSC Adv. 2016;6:65338.
31. Modreanu M, Nolan M, Elliott SD, Durand O, Servet B, Garry G, Gehan H, Huyberechts G, Papadopoulou EL, Androulidaki M, Aperathitis E. Optical and microstructural properties of p-type $SrCu_2O_2$: first principles modeling and experimental studies. Thin Solid Films. 2007;515:8624–31.
32. Stanciu I, Predoana L, Pandele Cusu J, Preda S, Anastasescu M, Vojisavljević K, Malič B, Zaharescu M. Thermal behaviour of the TiO_2 based gels obtained by microwaves assisted sol–gel method. J Therm Anal Calorim. 2017;130:639–51.
33. Shelyapina M, Zvereva I, Yafarova L, Bogdanov D, Sukharzhevskii S, Zhukov Y, Petranovskii V. Thermal analysis and EPR study of copper species in mordenites prepared by conventional and microwave-assisted methods J Therm Anal Calorim. 2018;134:71–9.